condensed matter

MDPI

Article

Possible Benefits from Phonon/Spin-Wave Induced Gaps below or above E_F for Superconductivity in High-T_C Cuprates

Thomas Jarlborg †

Department of Quantum Matter Physics, University of Geneva, 24 Quai Ernest-Ansermet, 1211 Geneva 4, Switzerland; thomas.jarlborg@unige.ch

† The author has retired.

Abstract: A phonon of appropriate momentum k_F will open a band gap at the Fermi energy E_F. The gap within the electronic density-of-states (DOS), $N(E_F)$, leads to a gain in electronic energy and a loss of elastic energy because of the gap-generating phonon. A BCS-like simulation shows that the energy gain is larger than the loss for temperatures below a certain transition temperature, T_C. Here, it is shown that the energy count can be almost as favorable for gaps a little below or above E_F. Such gaps can be generated by auxiliary phonons (or even spin- and charge-density waves) with k-vectors slightly different from k_F. Gaps not too far from E_F will add to the energy gain at the superconducting transition. In addition, a DOS-peak can appear at E_F and thereby increase $N(E_F)$ and T_C. A dip in the DOS below E_F will result for temperatures below T_C, which is similar to what often is observed in cuprate superconductors. The roles of spin waves and thermal disorders are discussed.

Keywords: cuprates; band structures; superconductivity

PACS: 74.20.-z; 71.20.Gj; 74.20.Pq

Citation: Jarlborg, T. Possible Benefits from Phonon/Spin-Wave Induced Gaps below or above E_F for Superconductivity in High-T_C Cuprates. *Condens. Matter* **2022**, *7*, 41. https://doi.org/10.3390/condmat7020041

Academic Editors: Andrea Perali and Sergio Caprara

Received: 27 August 2021
Accepted: 6 June 2022
Published: 11 June 2022

1. Introduction

Phonons and electron-phonon coupling, λ, is driving superconductivity in most "low-T_C" superconductors, such as some elementary metals, transition metal nitrides and carbides, A15-compounds, etc. The superconducting T_C for these materials has been calculated by the BCS equation [1], or by the strong-coupling McMillan form [2], and the resulting T_C's show a reasonable correlation with measured T_C's among many superconductors with low or intermediate T_C [3–7]. The high T_C in pressurized H_3S was predicted from such calculations even before the measured confirmation [8,9]. A large T_C needs a large λ and a large electronic density-of-states (DOS) at the Fermi energy, E_F. However, the T_C's in doped cuprates and pnictides are high despite a low DOS at E_F and $N(E_F)$, and this fact cannot be understood from the above-mentioned methods. Several ab-initio calculations for cuprates have shown that λ of the order 0.1 to 0.2 are not sufficiently large to explain the high T_C's of these materials [10]. A similar discrepancy between calculations and observations can be observed for superconducting low-T_C, low-DOS near-insulators such as doped diamond [11,12].

Here, we investigate how dynamic waves, in particular phonons, make peaks and dips in the DOS close to E_F, and how this can be helpful for superconductivity. Phonons with propagation of atomic distortions along the lattice induce variations of the electron potential ($W(r)$), which can deform the band structure so that a bandgap appears. The wave length of the potential perturbation determines the energy of the gap center, and the size of the gap depends on the amplitude of the variations of $W(r)$. The DOS is peaked on both sides of the gap. These features appear in the real band structure of cuprates [13] as well as in the nearly-free-electron model. Static displacements (and periodic distributions of dopants, see later) deform the electron potential in the lattice and can make DOS peaks at E_F too, but gaps

and flat bands are not spread isotropically over the whole Fermi surface. A static distortion means a new ground state without a possible gain of energy from a phonon excitation, but the T_C of a material with such distortions will be higher than for an undistorted material if $N(E_F)$ is enhanced. This result supports the proposal that superconductivity will be favored by Van Hove singularities, with peaks in the DOS emerging as a consequence of structural lattice incommensurate modulations at the nanoscale, associated with frozen charge- or spin-density waves, in complex cuprate superconductors [14–16].

2. Theory

The atomic displacements in a phonon are different for different sites depending on the type of atoms, the type of movements (transverse and longitudinal), and on the phonon wavelength [17]. The electron potential within a displaced atom will alter (mainly because of the Madelung part) compared to a not-moving atom at the node position of the phonon, etc., so that the potential has a perturbation ($W(r)$) along the direction (r) of the phonon wave. The wavelength of the phonon, with wave vector q, determines what part of the electronic band is susceptible to have a gap. If W is smooth enough to be described by a single Fourier component and if the electron band is free-electron like, then gaps appear at $\pm\frac{1}{2}q$ and the gap is 2V, where V is the maximal amplitude of W [18]. This is in one dimension, but complementary phonons with other directions of q will span the gap on a 3-dimensional Fermi surface. The movement of a single atom is almost harmonic with a restoring force proportional to the displacement. Assuming that the force constant is the same for each atom and that the direction of the displacements is irrelevant, then we can estimate that the elastic energy of the distorted lattice is Ku^2 per atom, where K is the (positive) force constant for each atom in the lattice and u is a representative averaged amplitude for all atomic displacements. A negative K for static displacements is not considered here. It depends on the electron-phonon coupling if a large u is able to make V large.

It is instructive to compare the energy required for a phonon distortion, Ku^2 (where K and u are the representative values for the force constant and the distortion amplitude, respectively), to the gain in electronic energy (also calculated per atom) because of the gap (V) generated by the phonon [19]. The gain is usually smaller than the elastic energy and no phonons will be excited. However, the opposite case is interesting when energy can be gained through the activation of phonon vibrations. The distortions u are repeatedly zero for optic phonons and their gaps can therefore fluctuate in time, at least for adiabatic conditions. Acoustic phonons can support stable gaps, since they always have non-zero displacements at some points along the atomic rows. A gap is opened in the DOS if the gain of kinetic electron energy from the activated phonon is larger than the cost from the atomic vibrations. For a free-electron band, this leads to the following equation, as was shown previously [19]:

$$\frac{Ku^2}{NV^2} = (\int f\epsilon d\epsilon - \int f\epsilon|\epsilon|/\sqrt{(\epsilon^2 - V^2)}d\epsilon)/V^2 = J(T,V) \quad (1)$$

where the energy limits in the integration J are $\pm\hbar\omega$ (the reach of λ), and the interval $-$V to +V is excluded. The DOS, N, is assumed to be constant, and $f(E_F, \epsilon, T)$ is the Fermi–Dirac occupation. The coupling parameter $\lambda = N(E_F)I^2/M\omega^2$, where M is an atomic mass, ω is a phonon frequency and I is the matrix element $< dW/du >$; the change in $W(r)$ is due to the displacement du. Furthermore, $M\omega^2 = K$, and $I = V/u$ (assuming I constant all over the Fermi surface, FS) for harmonic oscillations, and Equation (1) can be written $1/\lambda = J(T,V)$. The analytic solution for $T = 0$, when f is a step function and the gap is at E_F, is the same as the BCS result for the superconducting gap at $T = 0$; $V = 2\hbar\omega e^{-1/\lambda}$ [19]. The logarithm of the BCS equation for T_C is:

$$1/\lambda = ln(1.13\hbar\omega/T_C) \quad (2)$$

The numerical limit of the J integral for $V \to 0$ turns out to be very close to the logarithm in Equation (2). Thus, Equation (1) describes the logarithm of the BCS T_C equation [19]. (The perturbative derivation of Equation (1) has no self-consistent feedback, no strong coupling effects, and is based on pure band structure, but because the final result is like BCS, we can, if we wish, refer to the derivation of BCS for gaps at E_F.)

The advantage of a numerical solution is that a transition temperature for a gap below or above the chemical potential (or for a non-constant DOS) can be determined. Such solutions are different from the BCS result and their gaps below or above E_F are not associated with superconductivity, but they might appear anyway if the balance between the gap energy and the vibrational energy is favorable. The particle-hole channel in BCS remains open for gaps slightly aside E_F when $df(E_F, \epsilon, T)/dT$ is wide enough for finite T.

It is generally considered that λ is coming from coupling to phonons only, but coupling to spin-fluctuations can be considered from complementary corrections in the development [20–24]. Calculations for cuprates demonstrate that spin waves and electron-phonon coupling can enforce each other and produce deep pseudogaps [13]. The same equations as for electron-phonon coupling can be used with appropriate parameters for λ_{spin} instead of λ_{phon}, but quantitative results based on the local-spin density approximation (LSDA) are not satisfying, see later.

Charge-density waves (CDW) have been demonstrated to reduce the superconducting T_C and the superconducting gap at E_F [25]. The doping dependence of the superconducting gap versus the pseudogap in cuprates appears as a result of the competition between a superconducting gap and a CDW gap [26]. The potential and the charge in CDW can be modulated without distortions of the atomic positions, and they (as well as spin waves) can therefore exist at higher frequency than atomic vibrations. Formation of CDW is an interesting subject, but an estimate of a corresponding λ_{cdw} has not been made and such waves are not discussed here. Instead, we consider how waves with gaps *aside* E_F can lead to T_C-enhancements for certain temperatures and gap positions.

The FS's of the cuprates are quite 2-dimensional (2D) because of the weak electron interaction between different CuO-planes, and the FS takes an almost cylindrical shape at certain dopings [27]. This is in contrast to the complicated 3-dimensional (3D) multi-structured FS's in transition metals and most conventional superconductors. The FS for the 2D cuprate can be approximated by a free-electron band to give a circular FS with radius k_F, which is well adapted for the model calculation below or for wires of 1D superconductors [28]. Equation (1) describes a gap on a single (one dimensional) band from a phonon perturbation with a suitable k-vector, k. This requires (like in the application of BCS to real 3-dimensional bands) that phonons with other directions and amplitudes of k-vectors have to be included in order to follow a gap over the entire FS. All band structures have inversion symmetry, and a gap at k will also appear at $-k$. This fulfills one condition of nesting, even if other types of nesting are possible between different bands in multi-band materials.

3. Results

First, we consider the normal case when $k = k_F$ (the free electron band opens a gap at a zone boundary k_F) and the energy of the gap center coincides with E_F in order to determine the superconducting of T_C. The bold (green) line is in the equation. Figure 1 shows the result for $J(T)$ for a small value of V (1/2 meV) and $\hbar\omega = 100$ meV. For instance, a T_C of 5 meV requires a λ of about 1/3.

Now, consider ('auxiliary') phonons with gaps below or above E_F. Their J-solutions, shown in Figure 1, are very close to the green curve for intermediate λ, so that an energy gain is possible for temperatures just slightly lower than the superconducting T_C. (Here, T_C denotes the transition temperature for a gap at E_F, i.e. a superconducting gap, as well as the transition temperatures for non-superconducting gaps below or above E_F). This is because the Fermi–Dirac function decreases slowly over a wide energy range for sufficiently large T, and the exact position of a gap relative to E_F is not so important for the energy balance

between electronic and vibrational energies. At low T, when f is almost a step function, there is very little energy gain from gaps below or above E_F, and that is why the two curves turn down at low T_C in Figure 1. An auxiliary phonon can adjust its k-vector so that the gap will optimize its position relative to E_F for the best energy gain at a given T.

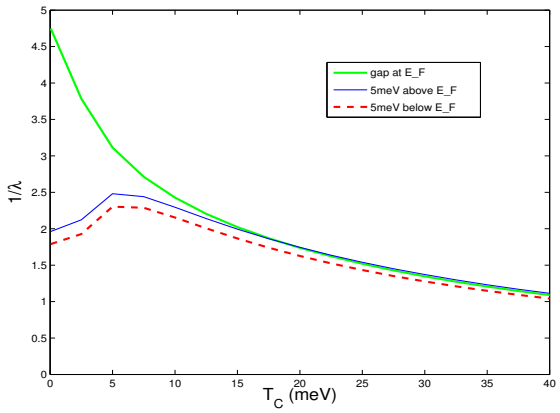

Figure 1. The result of T_C from Equation (1) with $V = 0.5$ meV for the gap at E_F (green heavy line), for the gap 5 meV above (thin blue line) and for 5 meV below (red broken line), E_F. Note that T_C is the transition temperature at which the (gain) of electronic energy equals the (cost) of vibrational energy for each of the three positions of the gap. This means that T_C is the superconducting gap for the gap at E_F, while the T_C's for the other two gap positions are just the temperature at which their respective gaps can appear. The blue and red curves in the figure will be pushed downwards if the gaps are more distant from E_F.

The separation between the blue and red curves in Figure 1 indicates that a gap above E_F has a larger energy gain than a gap below E_F. This is because E_F itself is pushed down together with the DOS peak induced by the gap above E_F (see Figure 2), and this increases the gain in kinetic energy. The situation is less favorable for a gap below E_F when the latter is pushed upwards by the gap. These effects due to the shift of the Fermi–Dirac edge are largest at low T and/or large gaps. A difference of the electric potential between a gapped and a normal region is possible if the two regions could be put together, similar to the thermo-electric effect.

Gaps aside E_F can enforce the superconducting gap at E_F. First, this is because of the positive energy count mentioned above. Secondly, these gaps appear at almost the same temperature as the superconducting transition and they generate a DOS peak at E_F with a higher $N(E_F)$. The energy spent on additional phonons will be paid back by a larger gain in electronic energy at a higher T_C. This second mechanism can widen a superconducting gap even as $T \to 0$, despite a negative energy count from the gaps. Phonons with gaps very far from E_F are not helpful, since no gain of kinetic energy is possible and since the DOS peaks are too far from E_F. A third mechanism to increase T_C is to generate a DOS-peak at E_F through a periodic distribution of dopants [16,29,30], but such a peak is fixed (no T-dependence) and the mechanism of energy gain is absent. The same can be achieved for a completely softened phonon (K negative) so that the distortions u become static. This can produce a DOS peak at E_F if the periodicity of the distortions in the lattice is optimal.

Figure 2 shows the un-broadened DOS function for a potential perturbation with $k > k_F$ and the resulting gap above E_F. Likewise, the gap appears below E_F if $k < k_F$. Figure 3 illustrates how two non-superconducting gaps of equal strengths below and above E_F are superimposed in a common DOS (without mutual interactions between the two gaps). The DOS has a sharp double peak near E_F, since the two gaps work against each other in the energy range near E_F. A stronger upper gap could push the DOS peak near E_F to lower energy, as was discussed above, and therefore lead to an additional energy gain. However, all phonon gaps near E_F probably have similar values of V/u and a symmetric DOS structure around E_F.

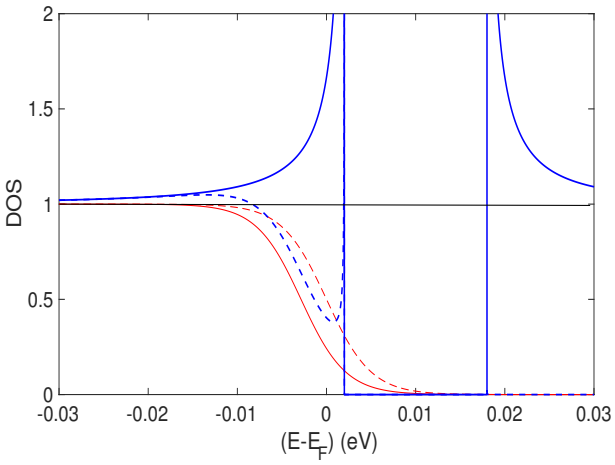

Figure 2. An example of how a free-electron DOS (the thin horizontal line) is deformed when a phonon sets up a periodic potential with a larger k-vector than k_F. A gap (here, of 16 meV) is then apparent above E_F (10 meV in this example shown by the bold blue line). The thin red line is the Fermi–Dirac distribution for the gapped DOS, and the broken bold blue line shows the occupied part of the DOS. The thin broken red line is the Fermi–Dirac distribution for the non-gapped DOS, which is equivalent to the Fermi–Dirac occupation of the constant DOS. As observed by the broken lines, the occupied Fermi–Dirac edge moves down by the presence of the gap above E_F. This leads to a gain in electronic energy, but the gain becomes smaller as T ($k_BT = 2.5$ meV in the plot) increases.

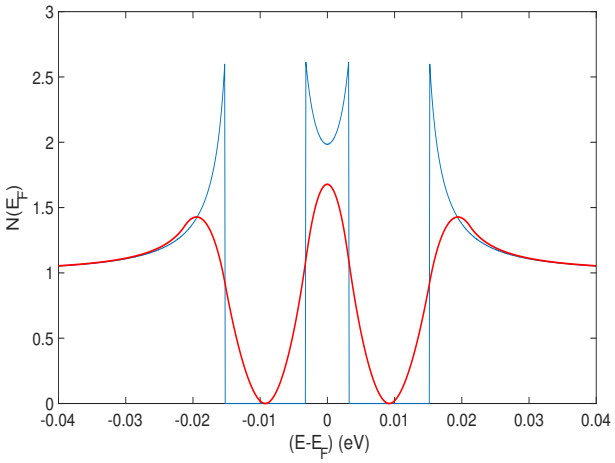

Figure 3. A model of how a constant DOS might be deformed when two phonons, one with k smaller than and one larger than k_F are present (thin blue line). Disorder can come from ZPM, thermal vibrations or spin-fluctuations, and has a smearing effect on the DOS with a large increase in $N(E_F)$ (bold red line).

Thermal disorder and zero-point motion (ZPM) of the lattice will smear the normal state DOS. This has been shown for several materials, where it can be detected [31–33] and be important for the physical properties in some materials [34–37]. The effect from disorder will also smear the gaps in normal-state DOS, and distort the DOS that surrounds the superconducting gap. The bold red line in Figure 3 shows the smeared two-gap DOS. The smearing (∼50 meV) is close to what is typical in other materials at low T from thermal disorder of the lattice, but effects of thermal spin disorder will add to the smearing. The smeared gaps remain as dips in the DOS, such as what is found from tunneling measurements in many cuprates [38], while the DOS is peaked at E_F.

4. Possible Spin-Waves

Band gaps at and being close to E_F require waves with almost the same wave length, and it is therefore tempting to believe that such waves are of different origin in order to minimize any destructing interaction between them. High-frequency spin waves and CDW are decoupled from slow phonon modes, but spin fluctuations can develop and follow the atomic distortions of a phonon. In fact, anti-ferro magnetic (AFM) fluctuations on Cu-sites and phonons are mutually enforced in cuprates if the waves have equal wavelengths, while different wavelengths generate gaps in the DOS at different energies (The Hamiltonian for calculating band gaps from phonons is obtained by having the atomic positions distorted (u) within a supercell. Instead, for band gaps from spin waves, the perturbations consist of having magnetic fields applied within the atomic spheres along the cell [13]). An AFM gap appearing below or above E_F will be stabilized by electronic energy gains as described above for phonons, but with an additional energy from the local (Ferro-magnetic, FM) spin splitting. The loss of elastic energy for phonons is replaced by a loss of kinetic energy when the electron gas is spin split. The Stoner condition for FM is that the gain of exchange energy ($N^2 I_s \xi^2$) has to be larger than the loss of kinetic energy ($N\xi^2$), where ξ is the spin splitting and I_s is an exchange integral [39–41].

FM spin-fluctuations are of interest if the two energies are approximately equal, but calculated values of the DOS and I_s in cuprates are too small for that. Observations of very weak FM moments in over-doped cuprates might be related to intrinsic disorder [42,43].

However, an AFM wave with alternating up and down spins along the lattice can, via the spin part of the potential, open a gap in the band structure of the two spins, similar to the effect of a potential modulation along a phonon distortion. The opening of gaps in the (two spin) DOS constitutes a gain in kinetic energy in addition to what might result from the local exchange-energy term, but as for phonons, the efficiency of these gains becomes weaker for gaps far from E_F. AFM and fluctuating AFM moments exist at moderate doping, but band calculations for cuprates based on the LSDA do not find AFM [10]. Simplified additions of higher spin-density gradients as well as kinetic energy corrections to the LSDA in band structure calculations show a stronger tendency towards AFM on Cu sites and make an opening of a weak gap in the band structure [44]. State-of-the-art inclusions of such corrections into what is called a meta-GGA potential [45], produce a stabilization of the magnetic moments on Cu in cuprates [46].

Calculations of the key parameters I_s and ξ by use of the meta-GGA potential for doped cuprates are needed to know whether AFM waves can be stabilized at a certain T and produce gaps in the DOS. Therefore, in the absence of such calculations, we cannot say if the superconducting gap and other gaps below and above E_F can be caused by pure phonons or spin-waves (or CDW), or whether the waves are mixtures between lattice distortions and magnetic excitations. Strong central peaks with weaker side spots have been detected by neutron scattering [47], which is an indication that complex magnetic interactions with different wavelengths might be present.

5. Conclusions

The message of this paper is that selected phonons, spin waves, or CDW, can generate partial gaps near E_F and thereby improve the conditions for a superconducting gap within a boosted DOS peak at E_F. Model calculations with reasonable values of the coupling demonstrate that a gap below or above E_F can appear at a temperature very close to the superconducting T_C. The superconducting gap and T_C can be boosted by these gaps through two effects: the increased gain of total energy from the side gaps and the higher $N(E_F)$. Auxiliary gaps appear and disappear together with the superconducting gap, and the energy position of the these gaps depend on the wavelengths of the generating waves. The wavelength is not fixed but can be modified so the gaps are able to find an optimized position as a function of T. This work has not demonstrated whether AFM spin-fluctuations (or CDW) are more likely than phonons to be responsible for gaps close to E_F.

Gaps produced by phonons have been discussed here because their coupling parameters are better known than for the other types of waves. Further works are needed to adress the questions about different types of waves as well as the energetics of the simultaneous opening of gaps at and aside E_F.

Funding: This research received no external funding.

Data Availability Statement: Not applicable

Acknowledgments: I am grateful to A. Bianconi for various discussions.

Conflicts of Interest: The author declares no conflict of interest.

References

1. Bardeen, J.; Cooper, L.N.; Schrieffer, J.R. Theory of Superconductivity. *Phys. Rev.* **1957**, *108*, 1175. [CrossRef]
2. McMillan, W.L. Transition Temperature of Strong-Coupled Superconductors. *Phys. Rev.* **1968**, *167*, 331. [CrossRef]
3. Gaspari, G.D.; Gyorffy, B.L. Electron-Phonon Interactions, d Resonances, and Superconductivity in Transition Metals. *Phys. Rev. Lett.* **1972**, *28*, 801. [CrossRef]
4. Papaconstantopoulos, D.A.; Boyer, L.L.; Klein, B.M.; Williams, A.R.; Moruzzi, V.L.; Janak, J.F. Calculations of the superconducting properties of 32 metals with $Z \leq 49$. *Phys. Rev. B* **1977**, *15*, 4221. [CrossRef]
5. Klein, B.M.; Papaconstantopoulos, D.A. Electron-Phonon Interaction and Superconductivity in Transition Metals and Transition-Metal Carbides. *Phys. Rev. Lett.* **1974**, *32*, 1193. [CrossRef]
6. Arbman, G.; Jarlborg, T. Trend studies of A15 compounds by self-consistent band calculations. *Solid State Commun.* **1978**, *26*, 857. [CrossRef]
7. Jarlborg, T.; Manuel, A.A.; Peter, M. Experimental and theoretical determination of the Fermi surface of V3Si. *Phys. Rev. B* **1983**, *27*, 4210. [CrossRef]
8. Li Y.; Hao, J.; Liu, H.; Li, Y.; Ma, Y. The metallization and superconductivity of dense hydrogen sulfide. *J. Chem. Phys.* **2014**, *140*, 174712. [CrossRef]
9. Drozov, A.P.; Eremets, M.I.; Troyan, I.A.; Ksenofontov, V.; Shylin, S.I. Conventional superconductivity at 203 kelvin at high pressures in the sulfur hydride system. *Nature* **2015**, *525*, 73. [CrossRef]
10. Pickett, W.E. Electronic structure of the high-temperature oxide superconductors. *Rev. Mod. Phys. B* **1989**, *61*, 433. [CrossRef]
11. Ekimov, E.A.; Sidorov, V.A.; Bauer, E.D.; Mel'nik, N.N.; Curro, N.J.; Thompson, J.D.; Stishov, S.M. Superconductivity in diamond. *Nature* **2004**, *428*, 542. [CrossRef]
12. Jarlborg, T. Theoretical aspects of simple and nested Fermi surfaces for superconductivity in doped semiconductors and high-T_C cuprates. *Solid State Commun.* **2014** *181*, 15–19. [CrossRef]
13. Jarlborg, T. Effects of spin-phonon interaction within the CuO plane of high-T_C superconductors. *Physica C* **2007**, *454*, 5–14. [CrossRef]
14. Perali, A.; Bianconi, A.; Lanzara, A.; Saini, N.L. The gap amplification at a shape resonance in a superlattice of quantum stripes: A mechanism for high Tc. *Solid State Commun.* **1996**, *100*, 181–186. [CrossRef]
15. Bianconi, A.; Valletta, A.; Perali, A.; Saini, N.L. Superconductivity of a striped phase at the atomic limit. *Phys. C Supercond.* **1998**, *296*, 269–280. [CrossRef]
16. Perali, A.; Innocenti, D.; Valletta, A.; Bianconi, A. Anomalous isotope effect near a 2.5 Lifshitz transition in a multi-band multi-condensate superconductor made of a superlattice of stripes. *Supercond. Sci. Technol.* **2012**, *25*, 124002. [CrossRef]
17. Kittel, C. Schematic figures of phonon displacements on individual atoms can be found in C. Kittel. In *Introduction to Solid State Physics*, 4th ed.; John Wiley & Sons: Hoboken, NJ, USA, 1971.
18. Ziman, J.M. *Principles of the Theory of Solids*; Cambridge University Press: New York, NY, USA, 1971.
19. Jarlborg, T. A model of the T-dependent pseudogap and its competition with superconductivity in copper oxides. *Solid State Commun.* **2011**, *151*, 639. [CrossRef]
20. Berk, N.F.; Schrieffer, J.R. Effect of Ferromagnetic Spin Correlations on Superconductivity. *Phys. Rev. Lett.* **1966**, *17*, 433. [CrossRef]
21. Fay, D.; Appel, J. Coexistence of p-state superconductivity and itinerant ferromagnetism. *Phys. Rev. B* **1980**, *22*, 3173. [CrossRef]
22. Jarlborg, T. Q-dependent stoner factors and reformulated spin-fluctuation enhancements: V and Pd. *Solid State Commun.* **1986**, *57*, 683. [CrossRef]
23. Monthoux, P.; Pines, D.; Lonzarich, G. Superconductivity without phonons. *Nature* **2007**, *450*, 1177. [CrossRef] [PubMed]
24. Jarlborg, T. Ferromagnetic and antiferromagnetic spin fluctuations and superconductivity in the hcp-phase of Fe. *Phys. Lett. A* **2002**, *300*, 518–523. [CrossRef]
25. Balseiro, C.A.; Falicov, L.M. Superconductivity and charge-density waves. *Phys. Rev. B* **1979**, *20*, 4457. [CrossRef]
26. Markiewicz, R.S.; Kusco, C.; Kidambi, V. Pinned Balseiro-Falicov Model of Tunneling and Photoemission in the Cuprates. *Phys. Rev. B* **1999**, *60*, 627. [CrossRef]
27. Damascelli, A.; Shen, Z.-X.; Hussain, Z. Angle-resolved photoemission studies of the cuprate superconductors. *Rev. Mod. Phys.* **2003**, *75*, 473. [CrossRef]

28. Mazziotti, M.V.; Jarlborg, T.; Bianconi, A.; Valletta, A. Room temperature superconductivity dome at a Fano resonance in superlattices of wires. *Europhys. Lett.* **2021**, *134*, 17001. [CrossRef]
29. Jarlborg, T. Mechanisms for higher T_C in copper oxide superconductors: Ideas from band calculations. *Appl. Phys. Lett.* **2009**, *94*, 212503. [CrossRef]
30. Jarlborg, T.; Bianconi, A. Multiple Electronic Components and Lifshitz Transitions by Oxygen Wires Formation in Layered Cuprates and Nickelates. *Condens. Matter* **2019**, *4*, 15. [CrossRef]
31. McKenzie, R.H.; Wilkins, J.W. Effect of Lattice Zero-Point Motion on Electronic Properties of the Peierls-Frohlich State. *Phys. Rev. Lett.* **1992**, *69*, 1085. [CrossRef]
32. Hedin, L.; Rosengren, A. On temperature broadening in X-ray spectra of metals. *J. Phys. F Metal Phys.* **1977**, *7*, 1339. [CrossRef]
33. Dugdale, S.; Jarlborg, T. Thermal disorder versus correlation in Compton profiles from alkali metals. *Solid State Commun.* **1998**, *105*, 283. [CrossRef]
34. Jarlborg, T. ϵ-FeSi: A material sensitive to thermal disorder. *Phys. Lett. A* **1997**, *236*, 143. [CrossRef]
35. Jarlborg, T. Role of thermal disorder for magnetism and the α-γ transition in cerium: Results from density-functional theory. *Phys. Rev. B* **2014**, *89*, 184426. [CrossRef]
36. Jarlborg, T.; Chudzinski, P.; Giamarchi, T. Effects of thermal and spin fluctuations on the band structure of purple bronze $Li_2Mo_{12}O_{34}$. *Phys. Rev. B* **2012**, *85*, 235108. [CrossRef]
37. Jarlborg, T.; Bianconi, A. Breakdown of the Migdal approximation at Lifshitz transitions with giant zero-point motion in the H_3S superconductor. *Sci. Rep.* **2016**, *6*, 24816. [CrossRef]
38. Fischer, Ø.; Kugler, M.; Maggio-Aprile, I.; Berthod, C.; Renner, C. Scanning tunneling spectroscopy of high-temperature superconductors. *Rev. Mod. Phys.* **2007**, *79*, 353. [CrossRef]
39. Stoner, E.C. Ferromagnetism. *Rep. Prog. Phys.* **1948**, *11*, 43.
40. Janak, J.F. Uniform susceptibilities of metallic elements. *Phys. Rev. B* **1977**, *16*, 255. [CrossRef]
41. Jarlborg, T.; Freeman, A.J. Magnetism and superconductivity in C15 compounds from self-consistent band calculations. *Phys. Rev. B* **1980**, *22*, 2232. [CrossRef]
42. Barbiellini, B.; Jarlborg, T. Importance of Local Band Effects for Ferromagnetism in Hole-Doped La2CuO4 Cuprate Superconductors. *Phys. Rev. Lett.* **2008**, *101*, 157002. [CrossRef]
43. Sonier, J.E. High-field muSR studies of superconducting and magnetic correlations in cuprates above Tc. *J. Phys. Cond. Matt.* **2010**, *22*, 203202. [CrossRef]
44. Jarlborg, T. Supercell Band Calculations and Correlation for High-TC Copper Oxide Superconductors. *Adv. Condens. Matter Phys.* **2009**, *2010*, 912067.
45. Sun, J.; Ruzsinszky, A.; Perdew, J.P. Strongly Constrained and Appropriately Normed Semilocal Density Functional. *Phys. Rev. Lett.* **2015**, *115*, 036402. [CrossRef] [PubMed]
46. Nokelainen, J.; Lane, C.; Markiewicz, R.S.; Barbiellini, B.; Pulkkinen, A.; Singh, B.; Sun, J.; Pussi, K.; Bansil, A. Ab initio description of the Bi2Sr2CaCu2O8+δ electronic structure. *Phys. Rev. B* **2020**, *101*, 214523. [CrossRef]
47. Tranquada, J.M.; Woo, H.; Perring, T.G.; Goka, H.; Gu, G.D.; Xu, G.; Fujita, M.; Yamada, K. Quantum magnetic excitations from stripes in copper oxide superconductors. *Nature* **2004**, *429*, 534. [CrossRef]